CCD PHOTOMETRY OF THE M87 JET

I. PÉREZ-FOURNON[1]
Instituto de Astrofísica de Canarias, La Laguna, Tenerife, Spain

L. COLINA[1]
Universitäts-Sternwarte, Göttingen

J. I. GONZÁLEZ-SERRANO
Instituto de Astrofísica de Canarias, La Laguna, Tenerife, Spain

AND

P. L. BIERMANN
Max-Planck-Institut für Radioastronomie, Bonn

ABSTRACT

CCD photometry of the M87 jet in the Thuan-Gunn r and g filters is presented. Accurate elliptical models of the underlying stellar emission were subtracted from the reduced and calibrated frames. The residual images show a number of morphological features not clearly seen before such as the faint extension at the end of the jet and faint red diffuse emission parallel to the jet on its northern side. The optical spectrum of the knots between the r and g bands is steeper than in the radio and, in general, becomes steeper with distance from the nucleus. The implications of this new result for particle acceleration mechanisms in jets are briefly discussed. The nondetection of a counterjet at an intensity level 300 times fainter than the jet places stronger constraints to relativistic beaming models of M87.

Subject headings: galaxies: individual (M87) — galaxies: jets — galaxies: photometry — shock waves — particle acceleration

I. INTRODUCTION

The jet in the giant elliptical galaxy M87 (NGC 4486, Virgo A, 3C 274) has been the subject of many studies at all frequencies (e.g., radio: Owen, Hardee, and Bignell 1980; Biretta, Owen, and Hardee 1983; IR: Stocke, Rieke, and Lebofsky 1981; optical: de Vaucouleurs and Nieto 1979; UV: Perola and Tarenghi 1980; and X-ray: Schreier, Gorenstein, and Feigelson 1982). It offers an unique opportunity to study in detail the physics of jets, particularly the mechanisms by which relativistic particles are accelerated to high energies (Webb, Drury, and Biermann 1984; Pérez-Fournon 1985; Pérez-Fournon and Biermann 1986; Biermann and Strittmatter 1987).

Recently, high spatial resolution imaging observations and image restoration techniques have revealed that the optical structure matches the radio one at the 0″.2 scale (Nieto and Lelièvre 1982; Lorre and Nieto 1984). Nevertheless, no absolute calibration is given in these high-resolution works. Previous absolute photometry (de Vaucouleurs and Nieto 1979) was obtained from photographic plates and had moderate spatial resolution. Furthermore, since the jet light is superposed on the inner part of M87 precise models of the underlying stellar emission are necessary to perform accurate photometry of the jet.

In this *Letter* we describe a method to construct elliptical galaxy models which accurately represent the underlying stellar light distribution, present CCD surface photometry of the jet, and give absolute fluxes and spectral indices for the different knots. Our results are the first measurement of optical spectral index variations along the M87 jet. Similar variations have been observed before in the 3C 273 jet by Röser and

Meisenheimer (1986). A new lower limit to the ratio of jet-to-counterjet intensities is given. The results are interpreted in terms of shock and relativistic beaming models of jets.

II. OBSERVATIONS AND DATA REDUCTION

The observations reported here were obtained with an RCA CCD camera at the Cassegrain focus of the 2.2 m telescope of the MPIA Calar Alto Observatory, Spain, on 1986 June 4. The corresponding angular scale and field of view are 0″.351 per pixel and $112'' \times 180''$, respectively. The seeing was 0″.95 FWHM, and the observing conditions were photometric. Two 5 minute exposures were obtained in each of the g and r filters of the Thuan-Gunn photometric system, with effective wavelengths 4930 Å and 6550 Å, respectively. The reduction technique consisted of bias subtraction and flat-fielding using exposures of the twilight sky. The two exposures in each passband were aligned and co-added to increase the signal to noise ratio. Absolute calibration was done from observations of standard stars of the list of Kent (1985). The magnitude to flux density conversion was taken from Cayatte and Sol (1987).

The program used to obtain accurate models of the galaxy light spatial distribution is a modified version of the ellipse fitting program PROF, contained in the GASP package written by M. Cawson and described in Davis *et al.* (1985). Before running PROF, contaminating objects and frame blemishes were identified and flagged in order to be avoided by the ellipse fitting procedure. Free parameters of the fit were ellipticity, position angle, and ellipse center for every given semimajor axis. The galaxy model was calculated by interpolation between the intensities of the fitted ellipses. The ratio between consecutive semimajor axes was constant, 1.059 ($\Delta \log = 0.025$) beginning at 4 pixels. The close spacing of consecutive fitted ellipses avoids strong interpolation errors. Sub-

---

[1] Visiting Astronomer, German-Spanish Astronomical Center, Calar Alto Observatory, operated by the Max-Planck-Institut für Astronomie.

traction of the elliptical galaxy model leaves a flat background. Its mean value differs from zero by less than about 0.1% of the underlying galaxy light.

The accurate galaxy light subtraction and good spatial resolution allow one to perform aperture photometry of the individual knots in the jet without large uncertainties in the background value. The photometry errors include the zero point error of the photometry, the Poisson noise of the light in the aperture before model subtraction, and the uncertainty of the local background determination. Since the jet knots are clearly resolved and present multiple components (see Nieto and Lelièvre 1982), we preferred to perfom aperture photometry rather than model fitting to measure the knot fluxes.

III. RESULTS AND DISCUSSION

Figure 1 (Plate L4) shows a gray-scale display of the smoothed residual r image. The g image is similar but of lower signal-to-noise ratio. A number of objects can be identified in the residual images including foreground stars, M87 globular clusters, a background galaxy (G1 in Fig. 1) probably belonging to the galaxy cluster behind M87 (Huchra and Brodie 1984), and the jet. The original PSF was estimated to have 0″.95 FWHM from Gaussian fits to the brightest globular clusters in the 2′ × 3′ field (unresolved at the distance of M87).

Figures 2 and 3 (Plate L5), obtained from the unsmoothed residual r image, show in more detail the jet structure. Compared with previous published high-resolution images of the M87 jet, these galaxy-subtracted images show a number of new features. The faint tail at the end of the jet is clearly resolved into at least two knots as has been previously suggested by Nieto and Lelièvre (1982). We refer to them as H and H′. It is unclear if the unresolved south spot in the last knot, H′, is associated with the jet or is a globular cluster. Comparison with an 18 cm MERLIN map (R. Spencer 1987, private communication) shows no resolved feature at that position but the radio tail coincides with the main body of the optical tail.

Another new and interesting morphological feature is the presence of faint (surface brightness of about 23.5 mag per square arcsec) red emission on the northern part of knots A, B, H, and H′ (see Fig. 3 ([Pl. L5]). A number of possible interpretations are suggested. First, it could be synchrotron emission from highly relativistic electrons which flow out of the jet or from relativistic particles in a cocoon of backflowing plasma. In these cases, one would expect to detect associated radio emission. Published VLA and MERLIN maps of M87 do not show radio emission at the position of these diffuse optical features, but they have lower dynamic range than our optical data. The detection of a cocoon is relevant for the theoretical interpretation of jets since this is one of the features which could help distinguish between magnetohydrodynamical and pure hydrodynamical jets (Clarke, Norman, and Burns 1986). Alternatively, the diffuse emission could be due to emission lines (Hα is included in the r filter). Note that some of the Hα filaments first studied in detail by Ford and Butcher (1979) are clearly detected in the red image (see Fig. 1). Spatial association of radio emission regions with extended narrow line emission regions has been found in a number of radio galaxies (see review by van Breugel 1986) and in Seyfert galaxies (Unger et al. 1987; Wilson 1987; Colina et al. 1987a, b; A. Campos-Aguilar and I. Pérez-Fournon 1988, in preparation).

Another new result of this work is the determination of the color of the individual knot complexes in the jet. The optical spectral index α ($S_\nu \propto \nu^{-\alpha}$) of the knots is in general larger than in the radio and different from knot to knot. There is a trend for the spectrum to become redder with distance from the nucleus (Fig. 4). Table 1 lists the magnitudes, fluxes, and spectral indices of different knots or knot complexes, and the distance from the nucleus along a radial line at a position angle of 291°. The distances correspond to the positions where aperture photometry was performed, centered at the peak of the knot emission, measured with a precision of 1 pixel. The transverse distance to the jet axis was assumed to be zero except for knots C, G, H, and H′ with transverse distances of 0″.35, 0″.35, −1″.23, and −1″.23, respectively. The fluxes were measured in circular apertures of 2″.8 diameter, except for the total emission of the A + B complex and the integrated jet value where a 6″.3 dia-
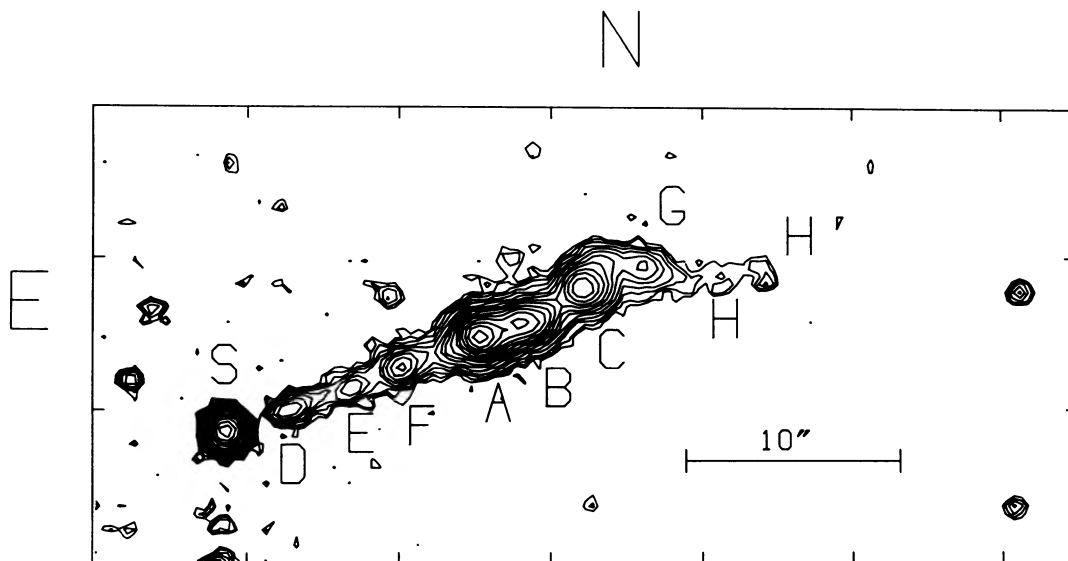
FIG. 2.—Isophotal map of part of the unsmoothed galaxy-subtracted image of M87 (r filter). First contour corresponds to 22.3 mag per square arcsec and the interval between contours is 0.35 mag. The jet knots discussed in the text and the stellar nucleus S are indicated.
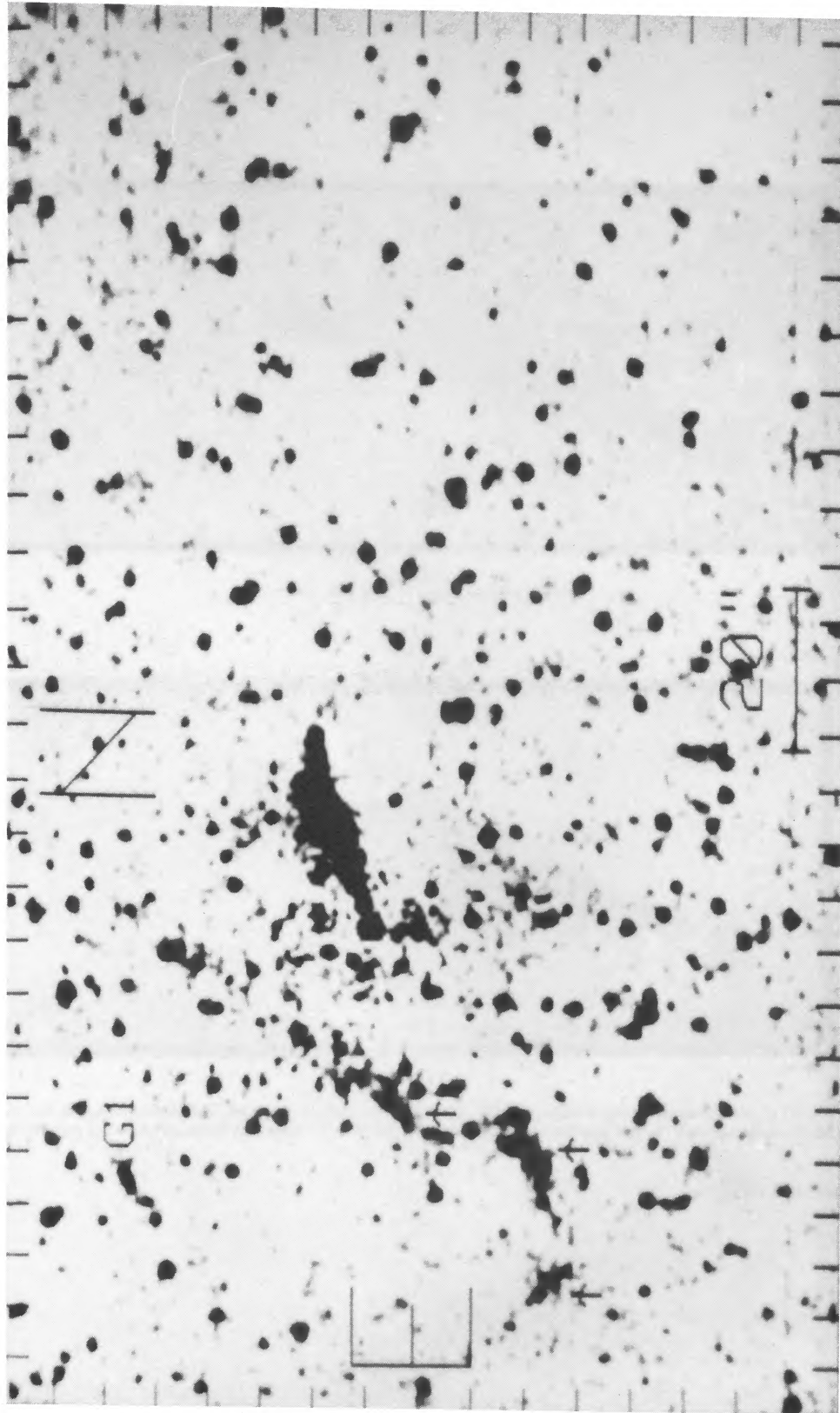
FIG. 1.—Gray-scale display of galaxy-subtracted image of M87 (r filter). A Gaussian filter of $\sigma = 1$ pixel (0".83 FWHM) was applied to be able to detect faint features. The arrows indicate some of the SE Hα filaments. The object labeled G1 is probably a background galaxy. No data are shown in a region of 25 pixels diameter at about 10' to the south of knot H' affected by a dust diffraction feature which could not be removed after flat fielding.

PÉREZ-FOURNON et al. (see **329**, L82)
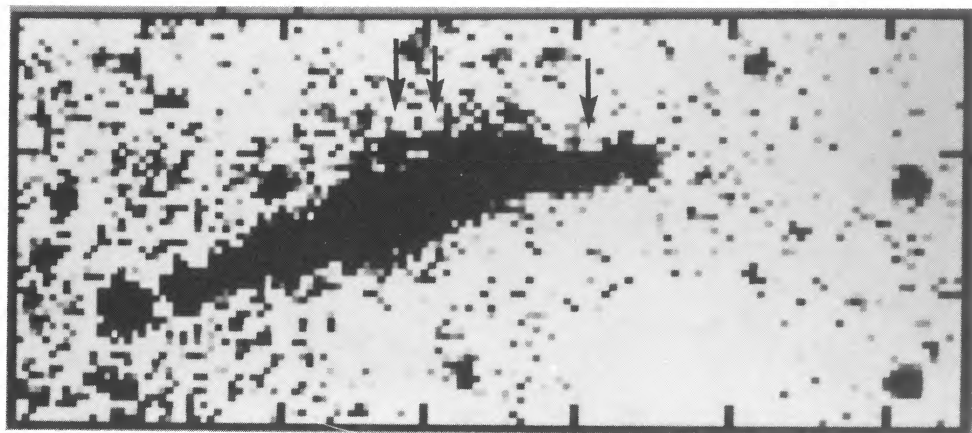
FIG. 3a
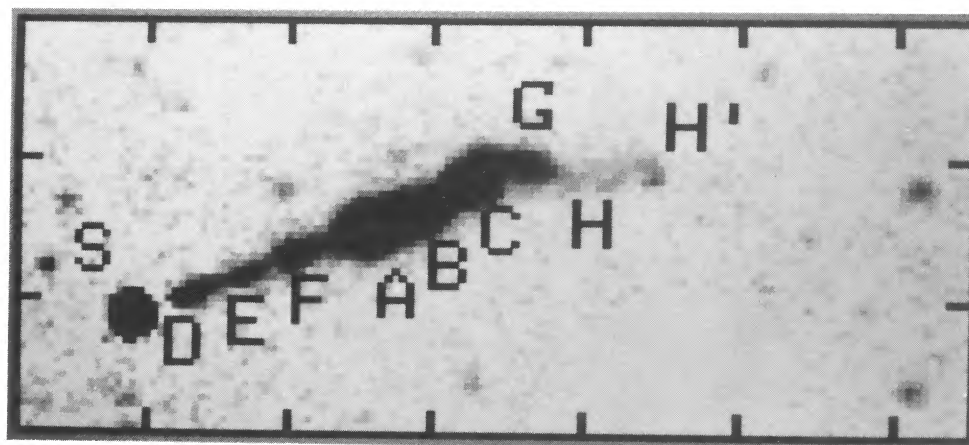
FIG. 3b

FIG. 3.—Gray-scale display of part of the galaxy-subtracted image of M87 (r filter) at different contrast. The faint diffuse emission on the northern part of the jet is indicated in (a), and the jet knots discussed in the text and the M87 nucleus S are labeled in (b). Note that the inner knots are resolved along the jet axis. The box size is 45″6 × 21″1.

PÉREZ-FOURNON et al. (see 329, L82)
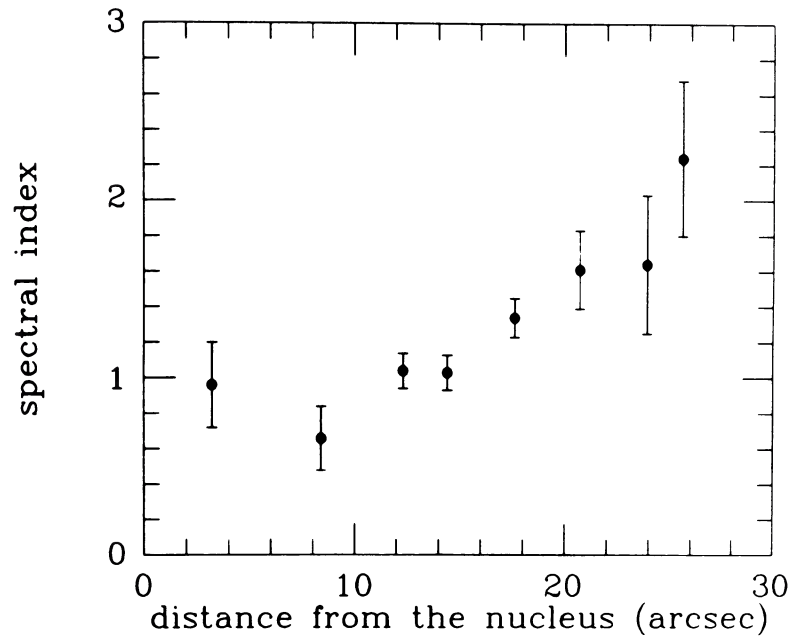
FIG. 4.—Optical spectral index between r and g of M87 knots D, F, A, B, C, G, H, and H' against distance from the nucleus along position angle 291°

meter aperture and a rectangular aperture of 26" × 5".6 centered on the jet axis were used, respectively. No values are given for knot E due to the low signal to noise ratio in the g band.

The steepening of the spectrum from the radio to the optical is consistent with a high-energy cutoff in the energy distribution of relativistic particles. Current shock acceleration models of jets (Pérez-Fournon and Biermann 1986; Biermann and Strittmatter 1987) predict an exponential decline of the spectrum in the optical range at frequencies higher than that characteristic of the highest energy electrons. The limitation of our observations to only two filters hinders a detailed analysis of the spectrum curvature. Previous data (reviewed by Keel 1984)

suggest that the IR-optical-UV spectrum of the jet becomes steeper with frequency. If this behavior persists at higher frequencies, the extrapolation to the X-ray range lies below the measured X-ray flux. This excludes synchrotron emission from a single power-law electron energy distribution as the X-ray emitting mechanism. A different electron population, such as derived from p-p collisions might explain the X-rays (Klemens 1987). Alternatively, the X-ray emission could be inverse Compton emission.

In the context of the model of Biermann and Strittmatter (1987) the gradual steepening of the optical spectral index can be understood as follows: These authors have argued that in parallel shocks first-order Fermi acceleration of electrons produces a universal cutoff frequency of the synchrotron emission of

$$v^* = 3 \times 10^{14}[3b(U/c)^2]f(a) \text{ Hz} , \qquad (1)$$

where $f(a) = (1 + Aa)^{1/2}/(1 + a)^{3/2}$, U is the shock velocity in the upstream plasma frame, b is the turbulent magnetic field energy density relative to the total magnetic field energy density, a is the photon energy density relative to the total magnetic field energy density, and $A \approx 200$ is a measure of the shape of the photon field, nearly independent of source parameters. At this frequency v^* the synchrotron emission of electrons shows a strong cutoff. The exact shape of this cutoff depends obviously on the shape of the cutoff in the electron energy distribution. The most extreme case is described by a power-law energy distribution with a Heaviside-step cutoff. Fitting the observed spectral indices to the synchrotron emission of a power-law electron energy distribution with a sharp cutoff then gives for each location along the jet the ratio of the observed frequency to the local cutoff frequency. Here we identify the cutoff frequency v_c as that frequency where the local spectral index is increased by unity from the power-law one of 0.57 (see Stocke, Rieke, and Lebofsky 1981). The resulting dependence of v_c on the distance x (in arcsec) along the jet can be fitted remarkably well by

$$v_c = 3.14 \times 10^{15} \exp\left[-(x - 3")/10".51\right] \text{ Hz} \qquad (2)$$

TABLE 1
OPTICAL PROPERTIES OF M87 KNOTS

Knot	Distance	m_r	m_g	S_r (μJy)	S_g (μJy)	Spectral Index[a]
D	3".2	19.08	19.12	103	78	0.96
		±0.05	±0.06	±4	±4	±0.24
F	8.4	18.72	18.66	144	119	0.66
		±0.03	±0.04	±5	±5	±0.18
A	12.3	16.51	16.57	1098	816	1.04
		±0.02	±0.02	±22	±17	±0.10
B	14.4	16.83	16.88	820	613	1.03
		±0.02	±0.02	±17	±13	±0.10
C	17.6	17.56	17.71	417	285	1.34
		±0.02	±0.03	±9	±7	±0.11
G	20.7	18.92	19.16	119	75	1.61
		±0.04	±0.06	±4	±4	±0.22
H	23.9	20.46	20.71	29	18	1.64
		±0.06	±0.10	±2	±2	±0.39
H'	25.6	20.47	20.91	29	15	2.24
		±0.06	±0.11	±2	±2	±0.44
A+B	13.3	15.87	15.86	1983	1566	0.83
		±0.02	±0.02	±40	±32	±0.10
Jet	...	15.40	15.38	3064	2448	0.79
		±0.03	±0.04	±97	±98	±0.18

[a] Spectral index α between the r and g bands. $S_v \propto v^{-\alpha}$.

with an error of $\sim 20\%$ in the scale in frequency and distance. It follows from our simple model that the observed cutoff frequency changes from $\sim 3 \times 10^{15}$ Hz to $\sim 4 \times 10^{14}$ Hz along the jet.

First, we have to check for the obvious effect of aging: Injecting high-energy electrons at a given location and transporting them along with velocity v in a magnetic field B ($\sim 10^{-3}$ G; Stocke, Rieke, and Lebofsky 1981) leads to a reduction of the critical frequency by a factor of 10 within 20 pc $(v/c)(B/10^{-3}$ G$)^{-3/2}$ corresponding to a fraction of an arcsec. Clearly, for an isotropic pitch angle distribution we require continuous reacceleration. The model of Biermann and Strittmatter (1987) proposes that this reacceleration takes place in repeated shocks along the jet, each emission knot corresponding to a shock structure. In the context of this model, several effects can change the frequency v^* ideally identical to v_c: (1) oblique shocks (see Jokipii 1987), (2) change of shock velocity, (3) nonnegligible photon field (i.e., $a \approx 1$), and (4) relativistic boosting. For simplicity we refer the following discussion to the standard case of $b = 1$, $(U/c)^2 = \frac{1}{3}$, and $a = 0$. We have to explain both the initially high cutoff frequency, 3×10^{15} Hz at $x = 3''$ and the gradual reduction of the cutoff frequency along the jet, to 3×10^{14} Hz at $x = 26''$.

Oblique shocks can increase the cutoff frequency by substantial factors for extreme angles between flow and shock-normal (in the shock frame where flow and magnetic field are parallel). An angle of 60° upstream increases the cutoff frequency by the required factor of order 10. Lacking a detailed theory for shock structures and their variation along a jet, we cannot pursue this possibility any further. Webb (1987) has demonstrated, that for $(U/c)^2 > \frac{1}{3}$, Fermi acceleration becomes inefficient and so the frequency cannot be increased at all. The photon energy density at $a = 0.5$ produces a cutoff frequency of 1.6×10^{15} Hz, a factor of ~ 2 short. The photon field energy density (i.e., the parameter a) has to decrease by a factor of order 100 to reduce v^* from 1.6×10^{15} Hz ($a = 0.5$) to 4×10^{14} Hz ($a = 0.005$) which is both insufficient and seems artificial. Relativistic boosting can readily accommodate factors of order 10, requiring bulk Lorentz factors γ_j of order 10 and angles to the line of sight θ of less than about 5°. In

order to explain the variation (at constant θ) of v_c along the jet, the bulk Lorentz factor has to decrease from values near 10 to values not far from unity. Combining relativistic boosting, nonnegligible photon fields and oblique shocks relaxes the limits on θ and γ_j considerably. We conclude that differential relativistic boosting along the jet is the simplest, but by no means unique, explanation for the variation of the cutoff frequency along the jet.

Low-luminosity radio galaxies usually present two-sided jets (Bridle and Perley 1984). The nondetection of a counterjet in M87 could be explained in two different ways: (1) the jet is close to the plane of the sky and intrinsically one-sided (Biretta et al. 1983), and (2) the jet is intrinsically two-sided, relativistic, and close to the line of sight. Our data allow a good determination of the lower limit of jet to counterjet ratio $R = 300$, larger than previous optical limits ($R = 100$; de Vaucouleurs and Nieto 1979) and comparable with the radio ones. At the VLBI scale $R = 200$ (Biretta et al. 1987). In the relativistic interpretation R can be expressed as

$$R = [(1 + \beta \cos \theta)/(1 - \beta \cos \theta)]^{2+\alpha}, \qquad (3)$$

where β is the jet bulk velocity in units of the velocity of light c, and θ is the angle between the jet axis and the line of sight.

Taking our measured value of the spectral index for the A + B complex and $R > 300$, we obtain $\beta \cos \theta > 0.76$. Further constraints to θ and β can be obtained from measurements of proper motions at the VLBI scale. Recent VLBI observations show that the apparent transverse velocity β_{obs} of individual features in the VLBI jet is subluminal, $\beta_{obs} = 0.34$ (Biretta et al. 1987). This is only compatible with a relativistically moving jet and $R > 300$ if $\beta_{obs} = \beta \sin \theta/(1 - \beta \cos \theta) = 0.34$ and $\beta \cos \theta > 0.76$. In the $\beta - \theta$ plane the allowed region reduces to the $\beta_{obs} = 0.34$ line with $\beta > 0.77$ and $\theta < 6°$, i.e., a relativistic jet at small angles to the line of sight.

REFERENCES

Biermann, P. L., and Strittmatter, P. A. 1987, *Ap. J.*, **322**, 643.
Biretta, J. A., Owen, F. N., and Hardee, P. E. 1983, *Ap. J. (Letters)*, **274**, L27.
Biretta, J. A., Reid, M. J., Junor, W., Spencer, R., and Muxlow, T. W. B. 1987, in *IAU Symposium 129, The Impact of VLBI on Astrophysics and Geophysics*, in press.
Bridle, A. H., and Perley, R. A. 1984, *Ann. Rev. Astr. Ap.*, **22**, 319.
Cayatte, V., and Sol, H. 1987, *Astr. Ap.*, **171**, 25.
Clarke, D. A., Norman, M. L., and Burns, J. A. 1986, *Ap. J. (Letters)*, **311**, L63.
Colina, L., Fricke, K. J., Kollatschny, W., and Perryman, M. A. C. 1987a, *Astr. Ap.*, **178**, 51.
———. 1987b, *Astr. Ap.*, **186**, 39.
Davis, L. E., Cawson, M., Davies, R. L., and Illingworth, G. 1985, *A.J.*, **90**, 169.
de Vaucouleurs, G., and Nieto, J.-L. 1979, *Ap. J.*, **231**, 364.
Ford, H. C., and Butcher, H. 1979, *Ap. J. Suppl.*, **41**, 147.
Huchra, J., and Brodie, J. 1984, *Ap. J.*, **280**, 547.
Jokipii, J. R. 1987, *Ap. J.*, **313**, 842.
Keel, W. C. 1984, *Ap. J.*, **279**, 550.
Kent, S. M. 1985, *Pub. A.S.P.*, **97**, 165.
Klemens, Y. 1987, Ph.D. thesis, University of Bonn.

Lorre, J. J., and Nieto, J.-L. 1984, *Astr. Ap.*, **130**, 167.
Nieto, J.-L., and Lelièvre, G. 1982, *Astr. Ap.*, **109**, 95.
Owen, F. N., Hardee, P. E., and Bignell, R. C. 1980, *Ap. J. (Letters)*, **239**, L11.
Pérez-Fournon, I. 1985, in *Active Galactic Nuclei*, ed. J. E. Dyson (Manchester: Manchester University Press), p. 300.
Pérez-Fournon, I., and Biermann, P. 1986, in *IAU Symposium 119, Quasars*, ed. G. Swarup and V. K. Kapahi (Dordrecht: Reidel), p. 405.
Perola, G. C., and Tarenghi, M. 1980, *Ap. J.*, **240**, 447.
Röser, H.-J., and Meisenheimer, K. 1986, *Astr. Ap.*, **154**, 15.
Schreier, E. J., Gorenstein, P., and Feigelson, E. D. 1982, *Ap. J.*, **261**, 42.
Stocke, J. T., Rieke, G. H., and Lebofsky, M. J. 1981, *Nature*, **294**, 319.
Unger, S. W., Pedlar, A., Axon, D. J., Whittle, M., Meurs, E. J. A., and Ward, M. J. 1987, *M.N.R.A.S.*, **228**, 671.
van Breugel, W. 1986, *Canadian J. Phys.*, **64**, 392.
Webb, G. M. 1987, *Ap. J.*, **319**, 215.
Webb, G. M., Drury, L. O'C., and Biermann, P. 1984, *Astr. Ap.*, **137**, 185.
Wilson, A. S. 1987, in *IAU Symposium 121, Observational Evidence of Activity in Galaxies*, ed. E. Ye. Khachikian, K. J. Fricke, and J. Melnick (Dordrecht: Reidel), p. 237.

P. L. Biermann: Max-Planck-Institut für Radioastronomie, Auf dem Hügel 69, D-5300 Bonn 1, Federal Republic of Germany

L. Colina: Departamento de Física Teórica, Universidad Autónoma de Madrid, Ciudad Universitaria de Cantoblanco, 28049 Madrid, Spain

J. I. González-Serrano and I. Pérez-Fournon: Instituto de Astrofísica de Canarias, 38200 La Laguna (Tenerife), Spain